normal subjects and 25 critically ill septic patients with bacteremia and sepsis-induced organ dysfunction. HMG-1 was not detectable in the serum of normal subjects, but significant levels were observed in critically ill patients with sepsis (Fig. 3), and these levels were higher in patients who succumbed as compared to patients with nonlethal infection.

HMG-1 is a highly conserved protein with >95% amino acid identity between rodent and human (*17–20*). It has previously been characterized as a nuclear protein that binds to cruciform DNA (*21*), and as a membrane-associated protein termed "amphoterin" that mediates neurite outgrowth (*19, 20*). Extracellular HMG-1 interacts directly with plasminogen and tissue type plasminogen activator (tPA), which enhances plasmin generation at the cell surface; this system plays a role in extracellular proteolysis during cell invasion and tissue injury (*19*). In addition, HMG-1 has been suggested to bind to the receptor for advanced glycation end products (RAGE) (*22*).

As with other inflammatory mediators such as TNF and IL-1, there may be protective advantages of extracellular HMG-1 when released in nontoxic amounts. Macrophages release HMG-1 when exposed to the early, acute cytokines, indicating that HMG-1 is also positioned as a mediator of other inflammatory conditions associated with increased levels of TNF and IL-1 (for example, rheumatoid arthritis and inflammatory bowel disease). Indeed, in most inflammatory scenarios, LPS is probably not the primary stimulus for HMG-1 release; it seems more likely that TNF and IL-1 function as upstream regulators of HMG-1 release. The delayed kinetics of HMG-1 release suggest that serum HMG-1 levels may be a convenient marker of disease severity. Moreover, the observations that HMG-1 itself is toxic, and that anti–HMG-1 prevents LPS lethality, point to HMG-1 as a potential target for therapeutic intervention.

References and Notes

1. K. J. Tracey *et al.*, *Science* **234**, 470 (1986); C. A. Dinarello, *FASEB J.* **8**, 1314 (1994); D. C. Morrison and J. L. Ryan, *Annu. Rev. Med.* **38**, 417 (1987); L. L. Moldawer, *Crit. Care Med.* **22**, S3 (1994).
2. B. Beutler, N. Krochin, I. W. Milsark, C. Luedke, A. Cerami, *Science* **232**, 977 (1986); J. W. Killion and D. C. Morrison, *Infect. Immun.* **54**, 1 (1986); A. Poltorak *et al.*, *Science* **282**, 2085 (1998).
3. K. J. Tracey *et al.*, *Nature* **330**, 662 (1987); M. Bianchi *et al.*, *J. Exp. Med.* **83**, 927 (1996); H. R. Alexander, G. M. Doherty, C. M. Buresh, D. J. Venzon, J. A. Norton, *J. Exp. Med* **173**, 1029 (1991); G. Wakabayashi, J. A. Gelfand, J. F. Burke, R. C. Thompson, C. A. Dinarello, *FASEB J.* **5**, 338 (1991).
4. D. G. Hesse *et al.*, *Surg. Gynecol. Obstet.* **166**, 147 (1988); H. R. Michie *et al.*, *N. Engl. J. Med.* **318**, 1481 (1988).
5. M. P. Fink, *Crit. Care Med.* **23**, 989 (1995); E. Abraham, *Chest* **113** (suppl.), 224S (1998).
6. M. W. Marino *et al.*, *Proc. Natl. Acad. Sci. U.S.A.* **94**, 8093 (1997); F. Amiot, C. Fitting, K. J. Tracey, J. M. Cavaillon, F. Dautry, *Mol. Med.* **3**, 864 (1997).
7. M. E. Bianchi, M. Beltrame, G. Paonessa, *Science* **243**, 1056 (1989); J. M. Walker, K. Gooderham, J. R. Hastings, E. Mayes, E. W. Johns, *FEBS Lett.* **122**, 264 (1980); L. Einck and M. Bustin, *Exp. Cell Res.* **156**, 295 (1985).
8. HMG-1 has also been termed "amphoterin" [J. Parkkinen *et al.*, *J. Biol. Chem.* **268**, 19726 (1993)]. HMG-1 and amphoterin are the same protein; we use the name "HMG-1" to reflect the original description of this protein as the first member of the HMG protein family.
9. HMG-1 was cloned by DNA amplification of the 648–base pair (bp) open reading frame from Rat Brain Quick-Clone cDNA (5 ng; Clontech, Palo Alto, CA) with the following primers: 5′-CCCGCGGATCCTCGAGGGAAGGATGGGCAAAGGAGATCCTA-3′ and 5′-CCCGCAAGCTTATTCATCATCATCATCTTCT-3′ (PCR at 94°C for 1 min, 56°C for 2 min, 72°C for 45 s; 30 cycles). The 680-bp PCR product was digested with Bam HI and Hind III and subcloned into the Bam HI–Hind III cloning sites of the pCAL-n vector (Stratagene, La Jolla, CA). The recombinant plasmid was transformed into *E. coli* BL21(DE3)pLysS (Novagen, Madison, WI), and positive clones were confirmed by DNA sequencing of both strands. Transformed cells were induced with isopropyl-D-thiogalactopyranoside, and rHMG-1 protein was purified with a calmodulin-binding resin column (Stratagene). As controls for experiments involving administration of rHMG-1 to mice, we purified proteins from *E. coli* BL21(DE3)pLysS that had been transformed with a plasmid that lacks the HMG-1 cDNA insert (pCAL-n). The amount of control material administered to mice was normalized to the number of *E. coli* that produce 0.5 mg of rHMG-1.
10. H. Wang and K. J. Tracey, unpublished observations.
11. Supplementary data can be found on *Science* Online at www.sciencemag.org/feature/data/1037699.shl.
12. Macrophages were obtained from the peritoneal cavity of LPS-sensitive (C3H/HeN and Balb/C) or LPS-resistant (C3H/HeJ) mice 4 days after intraperitoneal injection with 2.0 ml of thioglycollate broth (4%; Difco, Detroit, MI). Macrophages were pooled from four mice, resuspended into RPMI 1640, 10% fetal bovine solution (FBS), and 1% glutamine, and plated at a density of 4×10^6 cells per well in six-well Falcon Primaria tissue culture plates. After 24 hours, the culture medium was replaced with serum-free OPTI-MEM-I medium, and LPS (1 μg/ml) was added. The level of HMG-1 in the culture medium was determined 18 hours later by immunoblotting. HMG-1 was not detectable in culture medium of LPS-stimulated C3H/HeJ murine macrophages; HMG-1 levels reached 1 μg/10^6 cells in the culture medium of LPS-stimulated C3H/HeN murine macrophages.
13. L. B. Hinshaw *et al.*, *Circ. Shock* **30**, 279 (1990); C. Nathan and M. Sporn, *J. Cell Biol.* **113**, 981 (1991); D. G. Remick *et al.*, *Am. J. Pathol.* **136**, 49 (1990); R. E. Walker *et al.*, *J. Infect. Dis.* **174**, 63 (1996).
14. IgG was purified from anti–HMG-1 by Protein G–Sepharose HiTrap affinity chromatography (Pharmacia Biotech). Purified IgG fractions were desalted by ultrafiltration through Centricon-10 (Millipore), followed by two washes with 1× phosphate-buffered saline. The specificity of IgG was confirmed by immunoblot analysis of macrophage lysates, which revealed one band of 30 kD. Anti–HMG-1 IgG did not cross-react with LPS, TNF, IL-1, or bacterial proteins on immunoblots.
15. H. Wang and K. J. Tracey, unpublished observations.
16. M. P. Fink and S. O. Heard, *J. Surg. Res.* **49**, 186 (1990); K. J. Tracey, and E. Abraham, *SHOCK* **11**, 224 (1999); E. A. Deitch, *ibid.* **9**, 1 (1998).
17. K. L. Lee *et al.*, *Nucleic. Acids Res.* **15**, 5051 (1987); S. Ferrari, L. Ronfani, S. Calogero, M. E. Bianchi, *J. Biol. Chem.* **269**, 28803 (1994); S. Ferrari, P. Finelli, M. Rocchi, M. E. Bianchi, *Genomics* **35**, 367 (1996).
18. J. F. Maher and D. Nathans, *Proc. Natl. Acad. Sci. U.S.A.* **93**, 6716 (1996).
19. J. Parkkinen *et al.*, *J. Biol. Chem.* **268**, 19726 (1993).
20. M. Salmivirta, H. Rauvala, K. Elenius, M. Jalkanen, *Exp. Cell Res.* **200**, 444 (1992).
21. M. E. Bianchi and M. Beltrame, *Am. J. Hum. Genet.* **63**, 1573 (1998); D. Landsman and M. Bustin, *Bioessays* **15**, 539 (1993); M. Bustin and N. K. Neihart, *Cell* **16**, 181 (1979).
22. O. Hori *et al.*, *J. Biol. Chem.* **270**, 25752 (1995); A. M. Schmidt *et al.*, *Diabetes* **45**, S77 (1996).

23. We thank C. Dang for technical assistance; J. Eaton, J. Roth, B. Sherry, M. Bukrinsky, and M. Symons for critical reading of the manuscript; and D. Prieto for administrative assistance.

11 December 1998; accepted 3 May 1999

Ploidy Regulation of Gene Expression

Timothy Galitski,[1] Alok J. Saldanha,[1,2] Cora A. Styles,[1] Eric S. Lander,[1,2] Gerald R. Fink[1,2]*

Microarray-based gene expression analysis identified genes showing ploidy-dependent expression in isogenic *Saccharomyces cerevisiae* strains that varied in ploidy from haploid to tetraploid. These genes were induced or repressed in proportion to the number of chromosome sets, regardless of the mating type. Ploidy-dependent repression of some G_1 cyclins can explain the greater cell size associated with higher ploidies, and suggests ploidy-dependent modifications of cell cycle progression. Moreover, ploidy regulation of the *FLO11* gene had direct consequences for yeast development.

Changes in the number of chromosome sets occur during the sexual cycle, during metazoan development, and during tumor progression. Organisms with a sexual cycle double their ploidy upon fertilization and reduce their ploidy by half at meiosis. In the development of almost all plants and animals, specialized polyploid and polytene cell types arise though endocycles, cell cycles lacking cell division (*1*). Aberrant cell cycle control during tumor progression is thought to result in polyploidy and altered cell behavior (*2*).

Cells of different ploidy typically show very different developmental, morphological, and physiological characteristics. However, a lack

[1]Whitehead Institute for Biomedical Research, 9 Cambridge Center, Cambridge, MA 02142, USA. [2]Department of Biology, Massachusetts Institute of Technology, Cambridge, MA 02139, USA.

*To whom correspondence should be addressed. E-mail: fink@wi.mit.edu

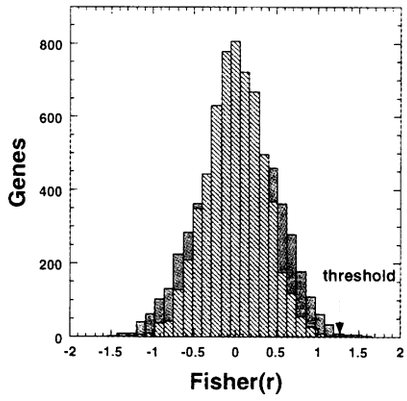

Fig. 1. Correlation thresholds. We compared correlation coefficients for experimental data and randomized data (within-gene permutations of experimental data) with a reference pattern proportional to ploidy. The hatched distribution shows the Fisher-transformed Pearson correlation coefficients, Fisher(r) = 0.5 ln[(1 + r)/(1 – r)], of a randomized data set. The variance of Fisher(r) for our randomized data (0.123) matched the theoretical variance of Fisher(r) under the null hypothesis for no correlation [n = 11, Var = 1/(n – 3) = 0.125]. The shaded distribution behind the hatched distribution represents Fisher(r) of experimental data against the reference pattern. A correlation threshold was set at Fisher(r) = 1.26 (r = 0.851), corresponding to 3.6 standard deviations of the random distribution. The same analysis was carried out for a reference pattern inversely proportional to ploidy [not shown; r = 0.858, Fisher(r) = 1.29, 3.7 standard deviations]. These thresholds should permit less than one false positive in the entire yeast genome.

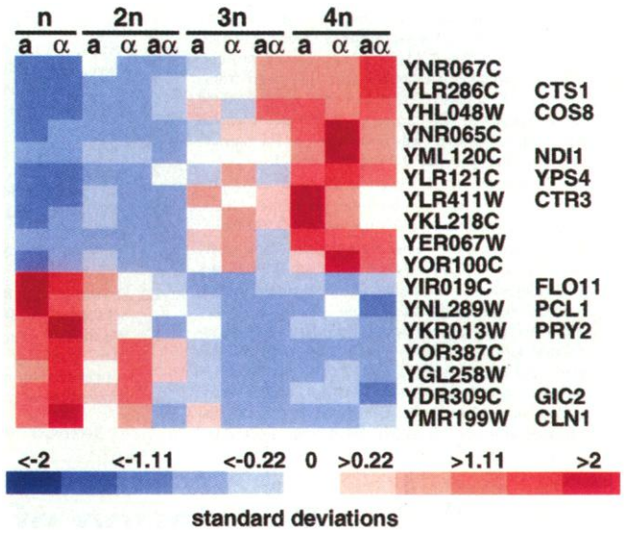

Fig. 2. Ploidy regulation. Ploidy-regulated genes are shown with color-coded expression levels normalized by standardization (mean = 0, SD = 1). The genes encoding known functions (*23*) are as follows: *CTS1*, endochitinase; *NDI1*, NADH-ubiquinone oxidoreductase; *YPS4*, GPI-anchored aspartyl protease; *CTR3*, high-affinity copper transporter; *FLO11*, cell surface flocculin; *CLN1* and *PCL1*, G_1 cyclins; and *GIC2*, control of actin cytoskeletal organization.

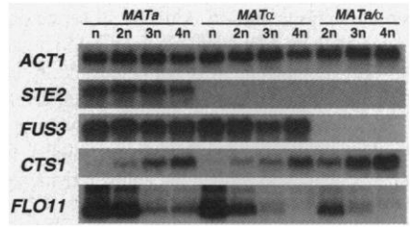

Fig. 3. Northern blot analysis of representative mRNAs, showing ploidy regulation of gene expression and mating-type control.

of isogenic controls obscures the contribution of ploidy to these differences. For example, in the yeast *Saccharomyces cerevisiae*, haploid cells of opposite mating type, *MAT***a** and *MAT*α, mate to produce a *MAT***a**/*MAT*α diploid. These three cell types have different phenotypes, many of which (such as mating, meiosis, and budding pattern) are directly attributable to their different genotypes at the mating-type locus rather than ploidy (*3*). However, one can parse the effects of mating type from those of ploidy by constructing isogenic sets of yeast strains that vary only in their ploidy, and then subjecting these strains to whole-genome expression analysis.

We generated an isogenic set of 11 strains varying in ploidy from haploid to tetraploid. There were three series, one for each mating-type genotype (*4*). Comparison of strains in which the mating type differs and ploidy is the same shows the role of mating type. Comparison of strains in which ploidy varies and the mating type is the same shows the effects of ploidy.

We looked for genes whose expression, relative to total gene expression, increased or decreased in proportion to ploidy. Using oligonucleotide-probe microarrays (*5*), we monitored the mRNA levels of all yeast genes in our strain set during exponential growth (*6*). We set two criteria (*7*) to identify ploidy-regulated genes: (i) There should be significant correlation with an idealized expression pattern either directly or inversely proportional to ploidy. Correlation thresholds were set such that random data are expected to produce less than one false positive in the entire genome (Fig. 1). (ii) Minima were set for relative and absolute changes in expression for each gene across all 11 strains. There were 17 genes satisfying both criteria; 10 were ploidy-induced and 7 were ploidy-repressed (Fig. 2) (*8*).

Ploidy-regulated genes showed substantial differences in expression within isogenic ploidy series. Comparing expression in haploids and tetraploids, *CTS1* was elevated by a factor of 12 and *FLO11* was repressed by a factor of 11. Ploidy-regulated genes had an unbiased distribution of locations in the yeast genome. They tended to have complex promoters; the average upstream intergenic space was longer than 1300 base pairs, whereas the genome-wide average intergenic space was 500 base pairs. The identities of some ploidy-regulated genes predicted specific ploidy-dependent cell type differences. For example, the ploidy-induced *CTS1* gene encodes a secreted endochitinase involved in the separation of mother cells and daughter buds; *cts1* mutants form large clumps of cells (*9*). Polyploids, with greater *CTS1* expression, were less clumpy than haploids (*10*).

Expression patterns uncovered by microarray data analyses were examined by Northern blot analysis of RNA samples (*11*) (Fig. 3). These results confirmed the existence of distinct ploidy-dependent and mating type–specific gene expression patterns. Most genes, like *ACT1*, showed no change in mRNA levels (relative to total RNA) in response to either ploidy or mating type. Of 32 mating type–specific genes [for example, *STE2* and *FUS3* (*10*)], none was among the ploidy-regulated genes of Fig. 2. Ploidy-regulated genes, such as *CTS1* and *FLO11*, showed ploidy-dependent expression regardless of the mating type. The magnitudes of the ploidy-dependent and mating-type effects observed in microarray experiments were in excellent agreement with quantitative phosphorimager analyses of Northern blots (*10*).

Measurements of the cells in our isogenic series demonstrated that cell size in yeast increases with increasing ploidy (Fig. 4). The association of increased ploidy with increased cell size has been observed in bacteria, fungi, plants, and animals (*1, 12*). The relation between cell size and ploidy could be explained by the fact that G_1 cyclins, Cln1 and Pcl1, are repressed as ploidy increases (Fig. 2). Yeast cells grow continuously during the G_1 phase and pass through START, the entry point into the cell cycle, at a cyclin-dependent critical size. Low expression of the G_1 cyclins results in START passage at a larger size; higher expression of G_1 cyclins results in START passage at a smaller size (*13*). According to this interpretation, the lower G_1 cyclin mRNA levels in tetraploids would cause them to pass through START at a larger size than haploids.

In addition to increased size, yeast cells

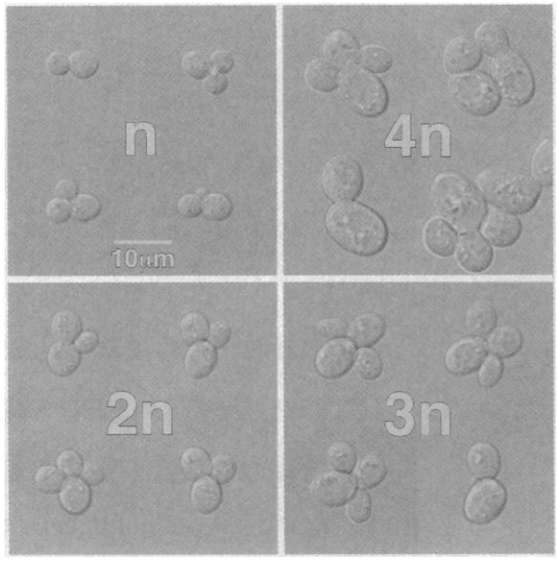

Fig. 4. Ploidy and cell morphology. Isogenic *MAT*α cells varying in ploidy from haploid (n) to tetraploid (4n) were sampled from exponential phase cultures (*6*) and observed with Nomarski optics. Morphological quantities (mean ± 95% confidence, $n = 50$) were calculated from length and width measurements of budded mother cells (the buds provided orientation) assuming rotational symmetry about the long axis. Cell volumes: haploid, 72 ± 1 μm³; diploid, 111 ± 2 μm³; triploid, 152 ± 3 μm³; tetraploid, 289 ± 6 μm³. Cell length/width ratios: haploid, 1.20 ± 0.01; diploid, 1.24 ± 0.01; triploid, 1.29 ± 0.01; tetraploid, 1.39 ± 0.02.

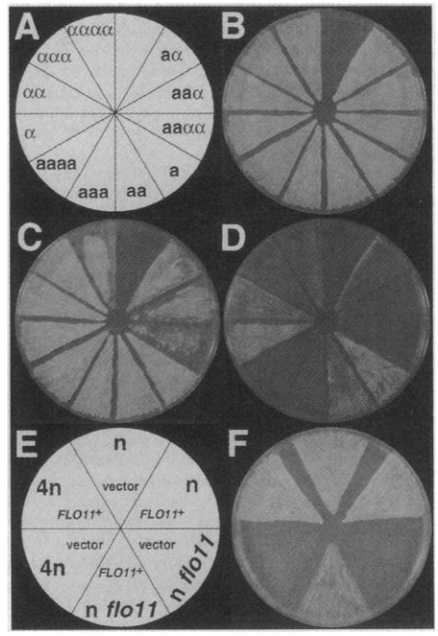

Fig. 5. Control of invasive growth by ploidy and mating type through *FLO11* expression. Invasive growth of strains [(**A**), genotypes] was visualized by washing the surface cells from a rich-medium petri plate with water (*16*). The plate is shown before washing (**B**), after a brief wash (**C**), and after extensive washing (**D**). A *FLO11*$^+$ multicopy plasmid, but not the vector plasmid (pRS202, 2 μm *URA3*), restores invasiveness to a haploid *flo11* null mutant (as a control) and to a tetraploid [(**E**), genotypes, all strains are *MAT***a**; (**F**), after washing].

showed greater elongation with increasing ploidy (Fig. 4). The basis for the connection between ploidy and morphology is suggested by ploidy-regulated genes. The ploidy-repressed Gic2 protein interacts with the Rho-type guanosine triphosphatase Cdc42. These proteins, along with Gic1, control actin organization and polarized cell growth, including bud site selection, bud emergence, and mating projection (shmoo) formation (*14*). Ynr067C is a ploidy-induced homolog (57% similar) of Acf2, a protein involved in polarized cortical actin assembly (*15*). The control of genes like *GIC2* and *YNR067C* suggests ploidy-dependent cytoskeletal organization.

Ploidy-dependent gene expression in yeast has important implications for the sexual cycle, development, and tumor biology. In mammalian cells, polyploidy in specialized cell types and hyperploidy in tumor cells may control cell physiology, morphology, and behavior. Although hyperploidy in tumor cells is usually viewed as a consequence of aberrant cell cycle control, altered ploidy may actually be a cause of altered cell properties.

We observed ploidy regulation of invasiveness, a developmental response in yeast. Invasive growth is a model for fungal virulence involving a change in budding pattern and the formation of chains of yeast cells that invade an agar substrate (*16*). On rich media, *MAT***a** and *MAT*α haploids exhibit much more vigorous invasive growth than *MAT***a**/α diploids (*16*). Haploid *flo11* mutants fail to invade, and overexpression of *FLO11* induces *MAT***a**/α diploids to invade more vigorously (*17*). Thus, Flo11, a serine-threonine–rich cell wall protein (*18*) whose molecular function is unknown, is a major determinant of this developmental response.

The ploidy repression of the *FLO11* gene was reflected in invasive growth (Fig. 5). As ploidy increased, the expression of *FLO11* and invasiveness decreased. In addition, *MAT***a**/α cells showed less *FLO11* expression (Figs. 2 and 3) and less invasiveness (Fig. 5, C and D) than did mating-type homozygotes of the same ploidy. Thus, ploidy (as well as mating type) governs this key developmental process.

The deficit of *FLO11* expression in cells of higher ploidy is directly connected with diminished invasion and is not simply a coincidental effect. A *FLO11* multicopy plasmid restored invasiveness to a tetraploid (Fig. 5, E and F). Thus, ectopic overexpression of *FLO11* can counteract the loss of invasiveness resulting from increased ploidy.

Patterns of gene expression associated with ploidy are not likely to be caused by alterations in growth rate or viability, or to be manifestations of differences such as the time of entry to diauxic shift during culture growth. For all of our strains, the exponential growth rates were similar and cell viabilities were greater than 95% (*6*). Expression patterns were monitored in cells at the same stage of exponential-phase growth. Furthermore, there is only one gene, *YER067W*, in common between the set of 17 ploidy-regulated genes and 98 genes induced or repressed early in diauxic shift (*19*).

There are several mechanisms by which gene transcription could respond to ploidy. Here we consider two: sensing gene dosage (*20*) and sensing total DNA content. In our ploidy series there are no changes in the dosage of any gene relative to other genes. However, the absolute number of each gene per cell is increasing and could be sensed by transient pairing of homologous chromosomes. Such transient pairing has been observed in humans, *Drosophila*, and *Saccharomyces* (*21*). Homologous pairing has been implicated in transvection, dominant position-effect variegation, and gene silencing, all of which involve alterations in gene expression (*22*). If pairing is responsible for ploidy-dependent regulation, then the presence of more homologs may increase the number of transient pairing interactions. Alternatively, the increase in the amount of DNA per cell presumably results in increased nuclear size and a reduction in the nuclear surface area/volume ratio. These changes may affect the import and nuclear concentration of regulatory proteins, which could result in the alterations in transcription we observe.

References and Notes

1. W. Nagl, *Endopolyploidy and Polyteny in Differentiation and Evolution: Towards an Understanding of Quantitative and Qualitative Variation of Nuclear DNA in Ontogeny and Phylogeny* (North-Holland, New York, 1978); I. Royzman and T. L. Orr-Weaver, *Genes Cells* **3**, 767 (1998).
2. E. C. Holland, W. P. Hively, V. Gallo, H. E. Varmus, *Genes Dev.* **12**, 3644 (1998); S. H. Bigner and J. Mark, *Prog. Exp. Tumor Res.* **27**, 67 (1984); A. M. Tahanda, J. M. Bruner, L. A. Donehower, R. S. Morrison, *Mol. Cell. Biol.* **15**, 4249 (1995).
3. M. A. Nelson, *Trends Genet.* **12**, 69 (1996); I. Herskowitz, J. Rine, J. Strathern, in *The Molecular and Cellular Biology of the Yeast* Saccharomyces*: Gene Expression*, E. W. Jones, J. R. Pringle, J. R. Broach, Eds. (Cold Spring Harbor Laboratory Press, Cold Spring Harbor, NY, 1992), pp. 583–656; G. F. Sprague and J. W. Thorner, ibid., pp. 657–744.
4. Isogenic strains were derived from *Saccharomyces cerevisiae* Σ1278b *MAT***a** *ura3-52 leu2::hisG his3::hisG*. Mating types were switched (for example, *MAT***a** to *MAT*α, and *MAT***a**/α to *MAT***a**/**a**) by transient expression

of the HO endonuclease from pGAL-HO. A brief exposure to galactose was followed by curing of pGAL-HO. Mating types were confirmed through mating and pheromone production assays. Matings produced the desired ploidy (for example, 2n *MAT***a**/**a** × 2n *MAT*α/α → 4n *MAT***a**/**a**/α/α). Ploidies of these zygotes were confirmed by tetrad dissections and analysis of mating-type segregation.

5. Total RNA was extracted and polyadenylated RNA was selected from cell samples. Using the methods of D. J. Lockhart *et al.* [*Nature Biotechnol.* **14**, 1675 (1996)] and L. Wodicka *et al.* [*ibid.* **15**, 1359 (1997)], we generated cDNA, produced biotin-labeled cRNA, hybridized fragmented cRNAs to high-density oligonucleotide arrays, stained with streptavidin-conjugated phycoerythrin, washed and scanned the arrays, and determined hybridization signal intensities, which are proportional to the target RNA concentration. Expression was measured as a trimmed average difference between 20 perfect-match and mismatch oligonucleotide probe pairs for each yeast gene. Scan-to-scan variations in intensity were corrected by a bulk scaling method analogous to adding equal amounts of total RNA to gel lanes in Northern blot expression analysis. For each scan, the sum of average differences was tallied. The median sum was found. The scaling factor for each scan (applied to each average difference in that scan) was the ratio of the median sum to the scan sum. All scaling factors were less than 2 and greater than 0.5. Scaled average differences ranged from ~0 to ~33,000; those less than 1 were set to 1.
6. All experimental cell samples were taken from asynchronous yeast cultures at late exponential phase (optical density at 600 nm = 1) growing in SC 2% glucose medium [F. Sherman, *Methods Enzymol.* **194**, 3 (1991)] at 30°C and 250 rpm. Samples were tested for viability by comparison of cell count with colony formation on plates as well as by staining with methylene blue. The growth of haploids and diploids was nearly indistinguishable. Triploids and tetraploids showed a 10 to 15% decrease in growth rates and an increased growth lag. *MAT***a**/α cells had a slight growth rate advantage and a shorter lag than their *MAT*-homozygous counterparts.
7. Expression data for each gene, as well as each reference pattern, were normalized to have mean = 0 and SD = 1. Pearson correlation coefficients were then calculated for each gene against a reference pattern either proportional to ploidy (haploids = 1, diploids = 2, and so forth) or inversely proportional (haploids = 1, diploids = 1/2, and so forth). The first criterion was that the correlation exceeded a threshold (Fig. 1). The second criterion was that the maximum and minimum average difference values for a gene differed by at least 100 units and at least a factor of 3. Ten random data sets (within-gene permutations of the experimental data set) showed that these criteria resulted in less than one false positive on average.
8. To download the data set, search the data, and view additional results, including an analysis of mating type–dependent expression, see http://staffa.wi.mit.edu/fink_public/ploidy/.
9. M. J. Kuranda and P. W. Robbins, *J. Biol. Chem.* **266**, 19758 (1991).
10. T. Galitski, A. J. Saldanha, C. A. Styles, E. S. Lander, G. R. Fink, data not shown.
11. Using the same total RNA samples used for microarray expression analysis, equal amounts of total RNA were added to each gel lane for Northern blot analysis. Radioactively probed mRNAs were visualized and quantitated by autoradiography and phosphorImager analysis. Total RNA samples derived from independent experiments (not shown) confirmed ploidy-dependent expression patterns.
12. R. K. Mortimer, *Radiat. Res.* **9**, 312 (1958); N. J. Trun and S. Gottesman, *Genes Dev.* **4**, 2036 (1990).
13. B. Futcher, *Yeast* **12**, 1635 (1996).
14. J. L. Brown *et al.*, *Genes Dev.* **11**, 2972 (1997); G. C. Chen, Y. J. Kim, C. S. Chan, *ibid.*, p. 2958.
15. T. Lechler and R. Li, *J. Cell Biol.* **138**, 95 (1997).
16. R. L. Roberts and G. R. Fink, *Genes Dev.* **8**, 2974 (1994).
17. W.-S. Lo and A. M. Dranginis, *Mol. Biol. Cell* **9**, 161 (1998).
18. ———, *J. Bacteriol.* **178**, 7144 (1996).
19. J. L. DeRisi, V. R. Iyer, P. O. Brown, *Science* **278**, 680 (1997).
20. M. Guo, D. Davis, J. A. Birchler, *Genetics* **142**, 1349 (1996).
21. B. M. Weiner and N. Kleckner, *Cell* **77**, 977 (1994); N. Kleckner and B. M. Weiner, *Cold Spring Harbor Symp. Quant. Biol.* **58**, 553 (1993).
22. B. T. Wakimoto, *Cell* **93**, 321 (1998); S. Henikoff and L. Comai, *ibid.*, p. 329.
23. Functional annotations are from the Yeast Protein Database (YPD) [P. E. Hodges *et al.*, *Nucleic Acids Res.* **27**, 69 (1999)].

24. We thank G. Acton, A. Dranginis, Q. Feng, T. Golub, M. Gordon, P. Hecht, F. Holstege, E. Jennings, F. Lewitter, H. Madhani, T. Ni, T. Orr-Weaver, J. Park, S. Rozen, D. Slonim, P. Tamayo, N. Watson, and R. Young for their contributions. Supported by Bristol-Meyers Squibb Company, Affymetrix Inc., and Millennium Pharmaceuticals Inc., and by NIH grant GM35010. G.R.F. is an American Cancer Society Professor of Genetics. T.G. is a postdoctoral fellow of the Helen Hay Whitney Foundation.

27 January 1999; accepted 13 May 1999

A Functional Assay for Centromere-Associated Sister Chromatid Cohesion

Paul C. Megee and Douglas Koshland*

Cohesion of sister chromatids occurs along the entire length of chromosomes, including the centromere where it plays essential roles in chromosome segregation. Here, minichromosomes in the budding yeast *Saccharomyces cerevisiae* are exploited to generate a functional assay for DNA sequences involved in cohesion. The centromeric DNA element CDEIII was found to be necessary but not sufficient for cohesion. This element was shown previously to be required for assembly of the kinetochore, the centromere-associated protein complex that attaches chromosomes to the spindle. These observations establish a link between centromere-proximal cohesion and kinetochore assembly.

The cohesion of replicated chromosomes (sister chromatids) is established near the time of DNA replication and persists until the metaphase-anaphase transition in mitosis. Cohesion proximal to the centromere on sister chromatids sterically constrains the centromeres so that they attach to microtubules emanating from opposite spindle poles. This ensures segregation of sister chromatids in opposition in the ensuing anaphase. In addition, the dissolution of cohesion is thought to be a key element in regulation of the metaphase-anaphase transition (*1*).

To understand the molecular basis of sister chromatid cohesion, it is necessary to identify and characterize the proteins and DNA elements important for this process. Proteins involved in cohesion have been identified and shown to be conserved from yeast to vertebrates (*2*–*4*). However, identification of requisite DNA elements has been thwarted by the fact that cohesion is not restricted to the centromere but occurs along the entire length of the chromosome (*5*, *6*). These observations suggest that cohesion factors may bind to chromosomes nonspecifically like histones or specifically to multiple sites. In either case, the DNA elements are functionally redundant, precluding their identification by classic genetic approaches.

The budding yeast is a powerful model system for analysis of DNA elements required for chromosome transmission because of the ability to construct 5- to 25-kb circular minichromosomes. Analysis of these minichromosomes led to identification of origins of replication

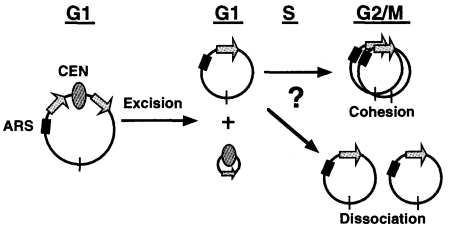

Fig. 1. Sister minichromatid cohesion assay. The minichromosome centromere (oval) is located between site-specific recombination sites (arrows). Black rectangle represents an *ARS*, the origin of replication. Hatch mark indicates the location of the test site used for mapping centromere-associated cohesion activity (see Fig. 4). Recombination results in excision of the intervening DNA, producing an acentric minichromosome and a minichromosome containing the centromere. Recombination (*8*) is induced in G_1-stage cells containing a minichromosome of interest, and cells are then released from the G_1 block. The extent of sister minichromatid cohesion on the larger, acentric minichromosomes was assessed microscopically in cells sampled after release from the G_1 block or after mitotic arrest.

Howard Hughes Medical Institute, Department of Embryology, Carnegie Institution of Washington, 115 West University Parkway, Baltimore, MD 21210, USA.

*To whom correspondence should be addressed. E-mail: koshland@mail1.ciwemb.edu